Silica Gel Template for Calcium Phosphates Crystallization

ARTICLE *in* CRYSTAL GROWTH & DESIGN · NOVEMBER 2009

Impact Factor: 4.89 · DOI: 10.1021/cg900702p

DOI: 10.1021/cg900702p

CRYSTAL GROWTH & DESIGN Article
XXXX, Vol. XXX
000–000

Silica Gel Template for Calcium Phosphates Crystallization

Michele Iafisco,[†,‡] Marco Marchetti,[†] Jaime Gómez Morales,[§] María Angeles Hernández-Hernández,[§] Juan Manuel García Ruiz,[§] and Norberto Roveri*[,†]

[†]*Dipartimento di Chimica "G. Ciamician", Alma Mater Studiorum Università di Bologna, Via Selmi 2, 40126 Bologna - Italy,* [‡]*Dipartimento di Scienze Mediche, Università del Piemonte Orientale, Via Solaroli 4, 28100 Novara - Italy, and* [§]*Laboratorio de Estudios Cristalográficos, IACT (CSIC-UGR), Edificio López Neyra, Avenida del Conocimiento, s/n 18100 Armilla - Spain*

Received June 23, 2009; Revised Manuscript Received July 30, 2009

ABSTRACT: Synthetic calcium phosphates exhibit good properties as biomaterials, such as biocompatibility, bioactivity, and osteoconductivity, and they have important applications in the fields of bone tissue engineering and orthopedic therapies. In this work, we performed an extensive characterization of the composite calcium phosphates/silica synthesized in gel by varying the pH and density of the silica solution. As a function of the pH values, brushite, octacalcium phosphate, hydroxyapatite, and monetite crystallization have been obtained, while changing the silica solution density the crystals are covered by different amounts of silica which results differently structured as a function of the pH. These materials have been analyzed using several experimental techniques (X-ray diffraction, differential scanning calorimetry, Fourier transform infrared spectroscopy, transmission electron microscopy, scanning electron microscopy, and field emission scanning electron microscopy). Large brushite crystals present amorphous silica both embedded within them and deposited on the crystal surfaces. The resulting calcium phosphate−silica composite is deposited as a powder, but it can be also easily molded into monolithic forms. The results of this study could be of significance in the field of biomaterials for considerable improvements of performance of bone implants in terms of osteointegration and in possible association to set up calcium phosphates−silica biocomposites.

Introduction

In recent years, the synthesis and characterization of biocompatible materials to be used in medicine have acquired a great deal of importance in material science and engineering.[1] Among them, calcium phosphates are prominent since they are the natural components in several human and animal mineralized tissues. In fact, hydroxyapatite (HA) represents approximately 70% of the weight of bone, 75% of dentine, and 95% of enamel. The mineral phase of bone and tooth is constituted of hydroxyapatite crystals with a length of about 100 nm, width of 20−30 nm, and thickness of 3−6 nm and having low crystallinity, crystalline surface disorder, and nonstoichiometric composition especially for the presence of carbonate ions in the crystal lattice.[2] Synthetic biomimetic calcium phosphates need to be prepared with similar morphology, dimensions, and structural and chemical characteristics of biological ones.[3] In fact, the excellent biological properties of calcium phosphates crystals, such as the lack of toxicity, inflammatory and immunity responses, and high bioresorbability can be significantly increased by improving their similarity to biological ones.[4] However, the most significant consideration to set up a third generation biomaterial is its bioactivity. A biomaterial with bioactive properties must stimulate cellular response and, in bone, it needs to form links between its surface and living tissue. In the case of HA and bone, on starting mineralized layer, the osteoblasts of living bone can proliferate and produce apatite and collagen, a process termed osteointegration. Recently, it has been shown that glasses of the type Na_2O-CaO-SiO_2 are materials that favor osteointegration. This is because they interchange Na^+ and Ca^{2+} ions on the silicate surface with protons in the surrounding fluid, a process that gives rise to Si−OH groups, which induce the nucleation of hydroxyapatite. The presence of Na^+ and Ca^{2+} ions also favors the nucleation of hydroxyapatite.[5,6] Preliminary in vivo experiments showed that grafting of maxillary sinus using nanostructured hydroxyapatite silica gel as only bone filler is a reliable procedure also in critical anatomic conditions and after an early healing period.[7]

Sol−gel technology is now widely used to produce hybrid materials because it has allowed overcoming the difficulty of using the classical silica glass-based biomaterials.[8,9] This difficulty was due to the high process temperature employed in traditional methods of synthesis and the subsequent difficulty of manipulating the internal microstructure of the matrix. Moreover, the physical characteristics (including density, pore size, and nanostructure) of the silica can be tailored by controlling the sol−gel reaction kinetics and in particular the relative rates of hydrolysis and condensation.[10]

On the basis of these considerations and the property of silicate matrices, we have investigated the possibility of coating synthetic calcium phosphates with porous silica layers, which could serve both to enhance their bioactivity and tune the biocomposite dissolution rate.

Here, we report a straightforward, low-temperature, template-based method of synthesizing an osteoconductive, hierarchically porous, multifunctional calcium phosphates/silica composite material by diffusion of Ca^{2+} ions through a metasilicate gel, set with phosphoric acid, at different pHs and densities of the silica solution. We highlighted the crystallization of different calcium phosphates phases and the covering silica differently structured as a function of the pH evidencing the emergence of a new generation of biomaterials that could induce the development of functional composite materials. In this field, the use of innovative processes to

*Corresponding author. E-mail: norberto.roveri@unibo.it; fax: ++ 39 051 2099593.

combine a graded architecture and chemical composition in association with different bioactive molecules might be promising.

Experimental Section

The gels were prepared in a glass vial having a diameter of 15 mm starting from solutions of sodium metasilicate (Aldrich, SiO_2 44−47% w/w) at 1.03 or 1.09 g/cm^3 density acidified with 1.2 M H_3PO_4 (Riedel-de Haen, 85% v/v). Ultrapure water (0.22 μS, 25 °C) was used. The sodium metasilicate solutions were prepared in nitrogen flow. Experiments were performed at pH values ranging from 5 to 11, using different amounts of phosphoric acid. The pH values of the metasilicate solution were measured, a few seconds after mixing it with phosphoric acid, using a Sentron IntelliCupFet probe. One milliliter of a 1.00 M $CaCl_2$ (Aldrich 98% w/w) solution was poured onto 1.00 mL of the gel and allowed to diffuse and react with the phosphoric acid used to set the silica gel. The diffusion process was carried out for 7 days and after that period the materials were washed twice with water, freeze-dried at −60 °C under a vacuum (3 mbar) for 12 h and well milled. An additional representative experiment was performed using the metasilicate solution at density 1.03 g/cm^3 and pH 9.38 without freeze-drying the resulting materials. The bigger precipitated crystals were used for dissolution experiments. The specimens were treated with 5 M NaOH.

The silica structure without calcium phosphates was monitored by FT-IR and DSC. The sodium metasilicate solutions at different densities (1.03 or 1.09 g/cm^3) were acidified with 1.2 M phosphoric acid at different pH values (ranging from 5 to 11) and washed twice with ultrapure water.

Different techniques were used to characterize the powders obtained from the above syntheses. Powder X-ray diffraction patterns were collected using a PanAnalytical X'Pert Pro equipped with X'Celerator detector powder diffractometer using Cu Kα radiation generated at 40 kV and 40 mA. The instrument was configured with a 1/32° divergence and 1/16° antiscattering slits. A standard quartz sample holder 1 mm deep, 20 mm high, and 15 mm wide was used. The diffraction patterns were collected within the 2θ range from 1.5° to 60° with a step size (Δ 2θ) of 0.017° and a counting time of 3 s.

The quantitative analysis of the crystalline phases was carried out using QUANTO,[11] a Rietveld[12,13] computer program for quantitative phase analysis of polycrystalline mixtures.

The infrared spectra were recorded in the wavelength range from 4000 cm^{-1} to 400 cm^{-1} with 2 cm^{-1} resolution using a Thermo Nicolet 380 FT-IR spectrometer. A powdered sample (approximately 1 mg) was mixed with about 100 mg of anhydrous KBr. The mixture was pressed at 10t pressure into 7 mm diameter discs. Pure KBr disk was used as blank.

Differential scanning calorimetric investigations have been carried out on dried samples using a DSC Q100 instrument (TA Instruments, New Castle, DE, USA). Heating was performed in nitrogen flow (25 mL/min) using an aluminum sample holder at a rate of 10 °C/min up to 300 °C. The initial weight of samples was around 5 mg.

Scanning electron microscopy (SEM) observations were done with a Philips XL-20 scanning electron microscope and with a Gemini-1530 field emission scanning electron microscope (FESEM). Transmission electron microscopy (TEM) investigations were carried out using a Philips CM 100 instrument (80 kV). The powdered samples were dispersed in water and then few droplets of the slurry deposited on holey-carbon foils supported on conventional copper microgrids.

Data are presented as mean value ± standard deviation (SD). Differences were considered statistically significant at a significance p level of 90%.

Results and Discussion

A series of calcium phosphate crystallization experiments have been performed into silica gels prepared from metasilicate solutions with two different densities and subsequently activated at several pH values in the range from 5.4 to 10.3 (Table 1). We did not carry out experiments using a 1.03 g/cm^3 metasilicate solution density at a pH higher than 11 because of the long gelation time. At the density of 1.03 g/cm^3 periodical precipitation calcium phosphates Liesegang rings[14] were observed. The number of these rings increased with the time and the distance between two consecutive rings increased toward going from the top to the bottom of the vial. On the contrary, using metasilicate solution with density of 1.09 g/cm^3, a continuous white precipitate through the vial was observed.

Table 1. Experimental Conditions of Metasilicate Gels Formation

metasilicate solution density (g/cm^3)	pH				
1.03	5.45	6.83	7.64	9.38	10.28
1.09	5.42	6.90	7.54	9.33	10.30

Structural Investigation of Calcium Phosphates. The powder X-ray diffraction patterns of the calcium phosphates precipitated in the gels at density 1.03 g/cm^3 as a function of the pH are reported in Figure 1. In the reported diagrams the background has been subtracted; thus, the two broad bands produced by the amorphous silica are absent. The marked peaks at 5° 2θ (100), 12° 2θ (020), and 26° 2θ (002) are the distinguishing reflections of the three main phases revealed: octacalcium phosphate ($Ca_8H_2(PO_4)_6 \cdot 5H_2O$; OCP), dicalcium phosphate dihydrate or brushite ($CaHPO_4 \cdot 2H_2O$; DCPD), and hydroxyapatite ($Ca_5(PO_4)_3OH$; HA), respectively. The other diffraction peaks which identify the same phases have been not labeled for clarity.

DCPD crystallizes in the monoclinic system and its crystal structure consists of chains of Ca^{2+} and PO_4^{3-} ions, each one arranged parallel to each other. Lattice water molecules are interlayered between the calcium and phosphate chains.[15] OCP has a layered structure involving apatitic and hydrated layers. The apatitic layers contain calcium and phosphate ions distributed in a manner similar to that for HA, while the hydrated layer contains lattice water and less densely packed calcium and phosphate ions.[12]

An important observation is that the diffraction peaks associated with the crystalline planes (020) of brushite and (002) of HA are more intense than those in the reference patterns (PDF files); this fact indicates a preferential orientation and/or growth of the crystals along the b and c axis of DCPD and HA, respectively. It is to note that while DCPD grows in the whole pH range and its presence is higher at low pH, the formation of HA takes place only at a pH higher than 7. At high pH values (9−10), the formation of OCP, the hydrated form and a precursor of hydroxyapatite is also observed.

Figure 2 shows the powder X-ray diffraction patterns of the crystalline phases crystallized in gels obtained from a metasilicate solution of density 1.09 g/cm^3 as a function of gel pH. Also in this case the amorphous background, produced by the amorphous silica, has been subtracted to facilitate the reading of the diffraction patterns. The peaks marked are those ones characteristic of OCP, DCPD, and HA at 5° 2θ (100), 12° 2θ (020), and 26° 2θ (002), respectively. In this set of experiments at the highest pH value, the preferential hydroxyapatite and OCP formation at the expense of brushite is observed. Also at this density the diffraction peaks associated with the reflections of the crystalline planes (020) of DCPD and (002) of HA indicate a preferential orientation of the crystals. The OCP crystallization appears evident only at a pH value higher than 10 even if the OCP presence is frequently associated with the HA crystallization.

The presence of monetite ($CaHPO_4$; DCP) the anhydrous form of DCPD, can be appreciated in the X-ray diffraction patterns of samples obtained using the metasilicate solution of density 1.09 g/cm^3 at pH values between 6 and 8.

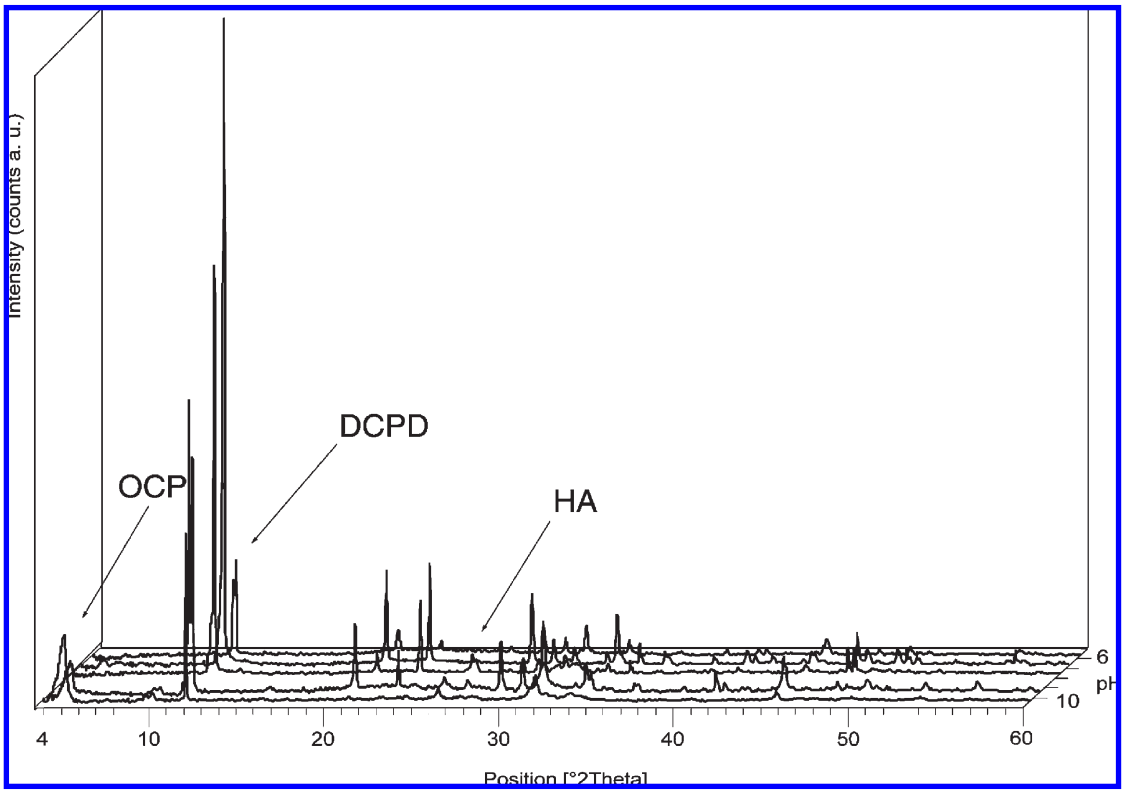

Figure 1. Powder X-ray diffraction patterns of the calcium phosphates obtained at different pH values of the silica gel prepared from metasilicate solution of density 1.03 g/cm^3.

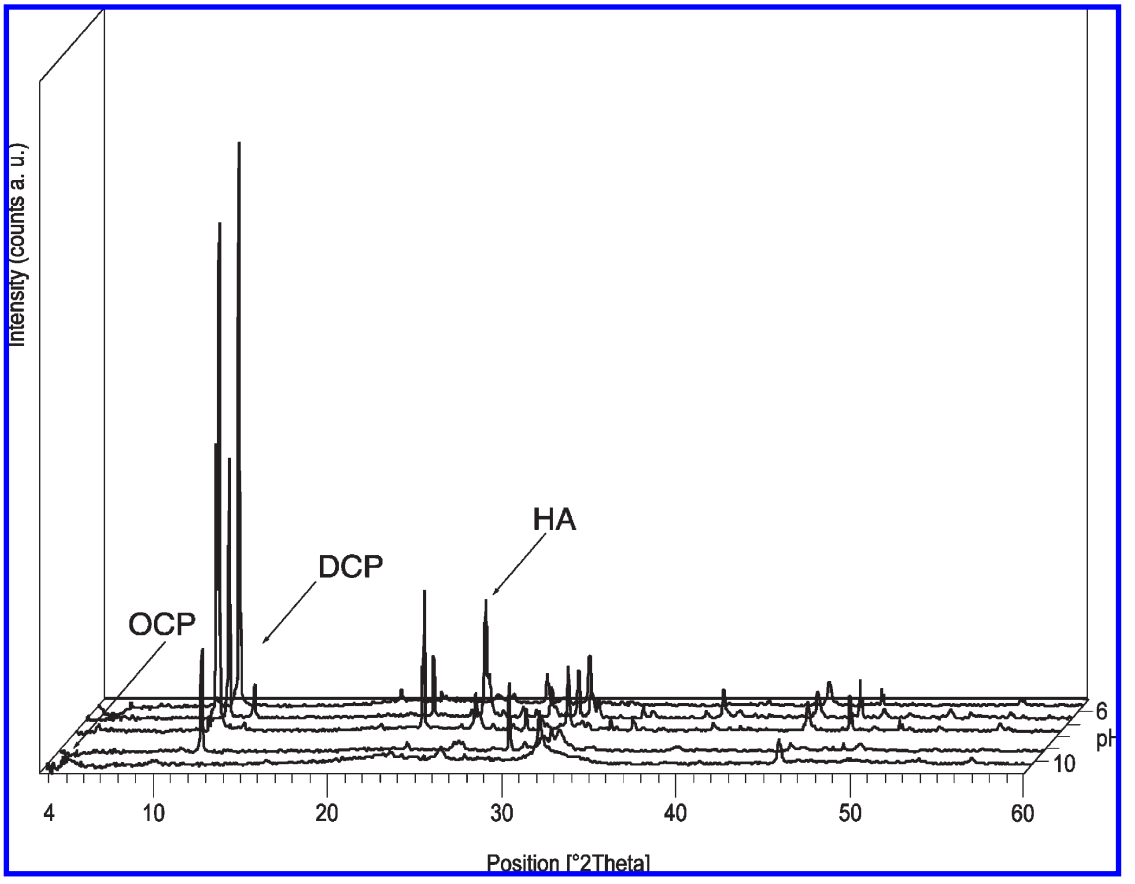

Figure 2. Powder X-ray diffraction patterns of the calcium phosphates obtained at different pH values of the silica gel prepared from metasilicate solution of density 1.09 g/cm^3.

Table 2. Weight Percentage (%) of each Calcium Phosphate Phase Calculated by Rietveld Refinement of Diffraction Patterns

metasilicate solution density (g/cm^3)	pH	DCPD (% wt)	HA (% wt)	OCP (% wt)	DCP (% wt)
1.03	5.45	100			
	6.83	100			
	7.64	70.3 ± 1.5	15.7 ± 5.4		
	9.38	66.1 ± 1.2	19.7 ± 4.4	14.2 ± 1.6	
	10.28	10.0 ± 0.9	23.4 ± 1.9	66.6 ± 0.4	
1.09	5.42	100			
	6.90	71.3 ± 4.7	18.1 ± 6.5		10.6 ± 1.5
	7.54	65.7 ± 8.1	24.3 ± 7.0		10.0 ± 2.9
	9.33	34.4 ± 0.9	65.0 ± 1.2		
	10.30		89.8 ± 0.9	10.2 ± 0.9	

The crystallographic structures of HA, DCPD, DCP, and OCP[16−19] were used as structural models for quantitative phases analysis in the Rietveld refinement of diffraction patterns. Profile fitting refinements were obtained by varying scale factor, background coefficient, profile function parameters, unit cell parameters, and preferential orientation of DCPD along (020) and HA along (002). Atomic thermal factors, site occupancies, and atomic positions were kept fixed during the refinement.

The percentage (% wt) of each calcium phosphate phase in the samples obtained at different conditions is reported in Table 2. It is noteworthy to note that after increasing the pH values the formation of hydroxyapatite increases at the expense of the brushite, a phase which preferentially forms close to neutral pH. Density values appear to strongly influence the crystallized phases and their relative amounts. In fact when increasing the pH from 5.4 to 10.3 the percentage of brushite phase decreases, whereas HA increases and this trend is sharp when the density was 1.09 g/cm^3. Furthermore, density values affect appreciably the HA/OCP percentage ratio which is higher at low density. Moreover, the formation of DCP takes place in the pH range from 6 to 8 using the metasilicate solution of density 1.09 g/cm^3 only. These findings suggest that the less dense gel favors the crystallization of OCP and DCPD which are the hydrated phases of HA and DCP, respectively. This behavior is due to the high amount of water entrapped in the structural pores of less dense gel.

Fourier transform infrared (FT-IR) spectroscopy has been utilized to investigate the same samples in order to clarify the conversion of DCPD into HA. FT-IR spectra of the samples obtained using the 1.03 g/cm^3 silica density and using the 1.09 g/cm^3 silica density as a function of pH values have been recorded in the wavelength region between 400 cm^{-1} and 700 cm^{-1} and are reported in Figure 3, panels A and B, respectively. Two peaks at 576 cm^{-1} and 528 cm^{-1} corresponding to the bending modes of the O−P−O bonds of the phosphate group of brushite (Figure 3 dotted lines) and two peaks at 561 cm^{-1} and 602 cm^{-1} corresponding to the bending modes of the O−P−O bonds of the phosphate group of hydroxyapatite (Figure 3 straight lines)[20] can be clearly observed. The transition from brushite to hydroxyapatite increasing the pH values clearly appears. In fact, when increasing the pH, the characteristic brushite bands disappear whereas the characteristic hydroxyapatite bands appear. The peaks characteristic of brushite at pH values higher than 10 can be observed only using the 1.03 g/cm^3 silica density, while they are absent using the 1.09 g/cm^3 silica density. These findings are consistent with the calcium phosphates phases detected by XRD.

Both DCPD and OCP have been implicated as possible precursors in the formation of apatite.[21] It has been demonstrated that under neutral or basic conditions the metastable phases brushite and OCP transform to HA through dissolution and reprecipitation processes, following the Ostwald rule of stages.[22]

The unexpected large amount of DCPD and OCP at starting basic pH values of silica solution is probably due to two important factors: the gel polymerization process and the calcium ions diffusion through the gel.[23,24] These two events, usually ignored in the crystallization in silica gels by ion diffusion, can perturb the local pH inside the gel and can create unpredictable zones at different pH. The diffusion of the concentrated calcium chloride solution in the gel decreases the pH at the front of crystallization. In fact, at the interface between gel and calcium chloride solution and in the gel close to this region a massive precipitation of very large brushite crystals (about 1 mm) takes place. In this zone, the pH is probably controlled by the calcium chloride solution. These effects appear to strongly influence the calcium phosphates phases grown in the gels.

Basically, the modulation of the growth parameters, such as metasilicate solution density and pH, allows different calcium phosphates phases to be obtained in agreement with previous research.

Structural Investigation of Dried Silica Gels. In order to investigate the structure and water content of silica and how these properties influence the calcium phosphates formation, the dried gels were studied by differential scanning calorimetry (DSC) and FT-IR.

The thermal analyses (Figure 4) revealed two endothermic peaks around 50 and 120 °C due to two different water losses, one imputable to the adsorbed water and the other one, at higher temperature, imputable to water entrapped into "funnel shaped" pores. When increasing the pH until 7, the temperature of the higher transition increased, whereas from pH 7 to 10 the temperature of the peak decreased, according to a modified silica structure.

This behavior is present in both silica gels set at different densities, but the second endothermic peak of silica set at 1.09 g/cm^3 (Figure 4b) shifts to temperatures below 100 °C. This is due to a weak interaction of silica with structural water in agreement with the reduced time of gelation of this material. In fact, the silica gelation time was a few seconds using metasilicate solutions with 1.09 g/cm^3 density, while using metasilicate solutions at 1.03 g/cm^3 density, the gelation time ranges from a few minutes (pH 5.45−6.83) up to one day (pH 9.38−10.28).

The general effect of the pH during gel synthesis on the pore structure and morphology has been extensively studied.[27] Changes in solution pH alter the relative rates of hydrolysis and condensation, yielding products ranging from weakly branched to particulate silica sols. The polymerization process can be divided into two approximate pH domains: pH 2−7 and pH > 7. pH 7 appears as a boundary because the silica solubility and dissolution rates are maximized at or above pH 7. The kinetics and growth mechanisms of the silica depend on the pH value of the mother solution. At acidic pHs, particle growth stops as soon as the size of 2−4 nm is reached. Above pH 7, particle growth is mainly dependent on the temperature, and particles of more than 100 nm in diameter can be formed. Above pH 7, particles are negatively charged, repel each other, and no aggregation of particles occurs. At low pH, repulsive forces

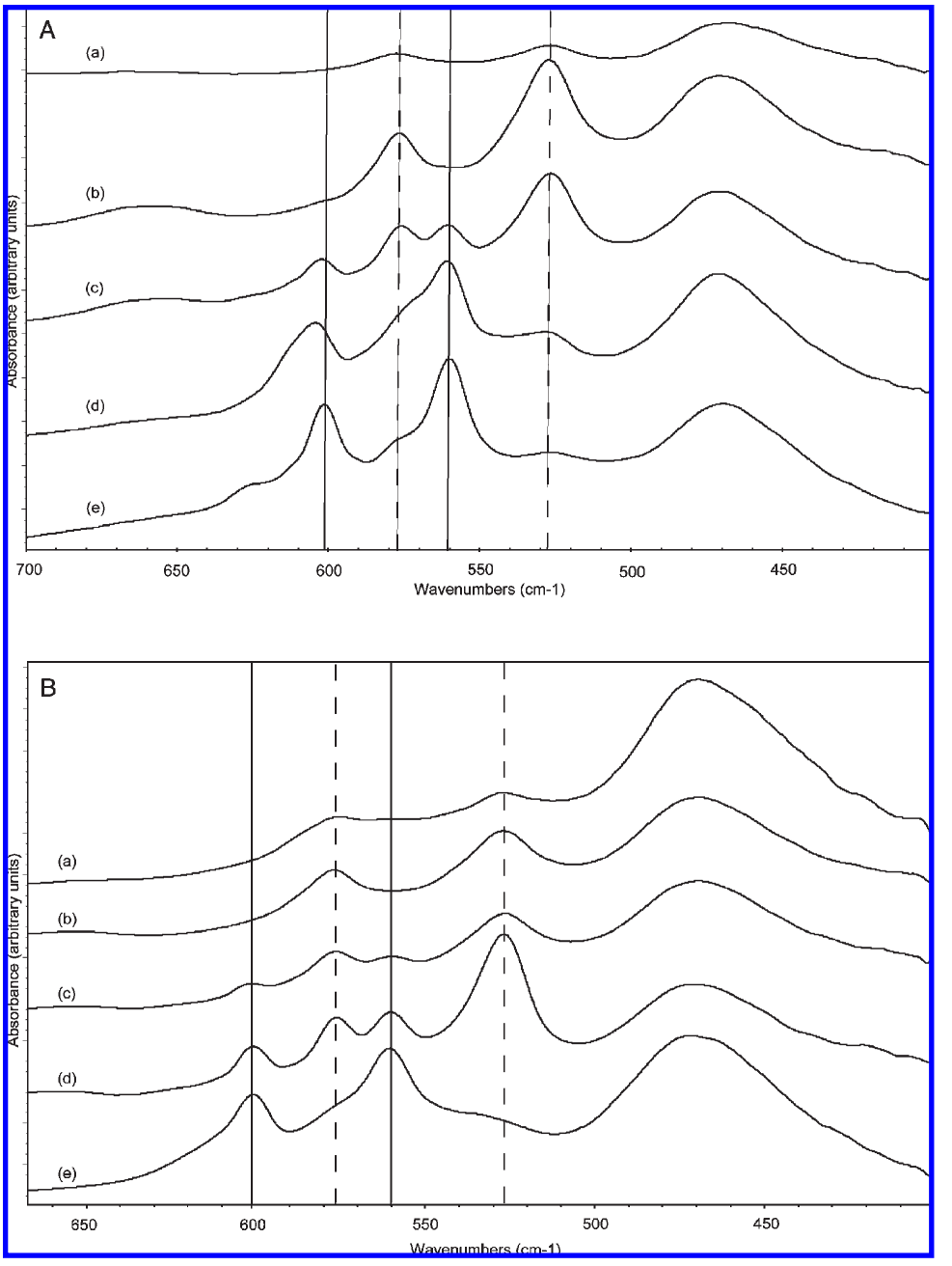

Figure 3. FT-IR spectra of the samples obtained at pH 5.45 (a), 6.83 (b), 7.64 (c), 9.38 (d), 10.38 (e) (density 1.03 g/cm^3) (A) and pH 5.42 (a), 6.90 (b), 7.54 (c), 9.33 (d), 10.30 (e) (density 1.09 g/cm^3) (B). The peaks at 561 cm^{-1} and 602 cm^{-1} correspond to the bending modes of the O−P−O bonds of the phosphate group of hydroxyapatite (straight lines). The peaks at 576 cm^{-1} and 528 cm^{-1} correspond to the bending modes of the O−P−O bonds of the phosphate group of brushite (dotted lines).

between particles are weak, particles collide and form continuous networks leading to gels.[22]

The relative rates of hydrolysis and condensation effectively determine the morphology of the final silica. Generally, silica particles are positively charged at low pH and negatively charged at high pH. At the isoelectric point of silica (between pH 1 and 3), where the electrophoretic mobility of particles is zero, or at the point of the zero charge, the condensation rate is the lowest.[28] The weakly basic and moderate acidic sols have significant amounts of deprotonated silanol groups (SiO^-), which increase the condensation rate causing the formation of highly branched silica species. Gelation of these branched species results in the formation of mesoporous regions with a pore size between 2 and 50 nm.[28]

As the pH is lowered to reach the isoelectric point (between 1 to 3), the gelation times are increased accordingly as in the basic sol, and this leads to linear or randomly branched silica gel having in this case highly microporous structure with a pore diameter <2 nm. At very high acid concentrations, below isoelectric point (<1), the dried gels become more mesoporous. This is due to the protonation of silanols that produce ($SiOH_2^+$) groups, which are good leaving groups and act to increase the rate of condensation.[29,30]

The evolution of the silica structure was monitored by FT-IR spectroscopy. In fact, infrared spectroscopy has been employed over the last three decades to investigate the structure and the defects on the chemical structure of silica gels. The 1080 cm^{-1} band has been largely used to obtain

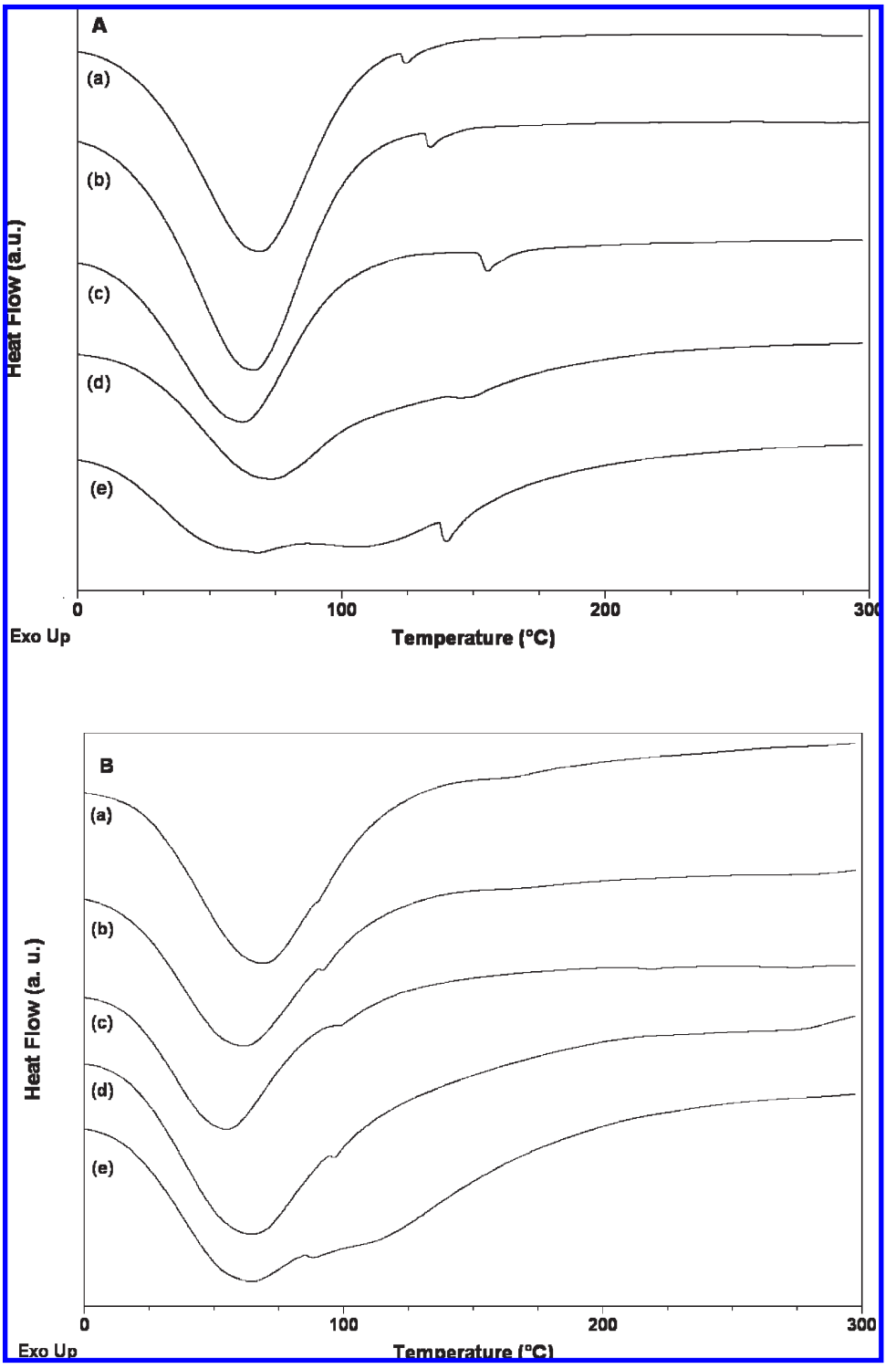

Figure 4. DSC curves of the dried silica obtained at pH 5.45 (a), 6.83 (b), 7.64 (c), 9.38 (d), 10.38 (e) (density 1.03 g/cm^3) (A) and pH 5.42 (a), 6.90 (b), 7.54 (c), 9.33 (d), 10.30 (e) (density 1.09 g/cm^3) (B).

information on the Si−O−Si bond tensile strain (angle and length), porosity, and density of silica.[31,32]

The spectra (Figure 5) recorded in the wavenumber region between 1400 cm^{-1} and 800 cm^{-1} show a broad peak at 1080 cm^{-1} due to the asymmetric stretching of Si−O−Si and a peak at around 950 cm^{-1} due to the stretching of Si−OH.[33]

The Si−O−Si stretching vibration band can be deconvoluted in four or five peaks at around 1055 cm^{-1}, 1110 cm^{-1}, 1160 cm^{-1}, 1080 cm^{-1}, 1200 cm^{-1}.[34] According to the literature,[35] the 1080 cm^{-1} and 1055 cm^{-1} peaks correspond to transversal optical (TO) and longitudinal optical (LO) asymmetric stretching modes of Si−O−Si, respectively. The silica structure contains cyclic and linear structures.[31] We assigned the 1080 cm^{-1} and 1200 cm^{-1} vibrations of Si−O−Si to cyclic structures. The other peaks at 1050 cm^{-1}, 1100 cm^{-1}, and 1160 cm^{-1} have been assigned to stretching vibrations of Si−O−Si belonging to a more linear, less cross-linked structure.[34] It is clear that the wavenumbers of the bands at

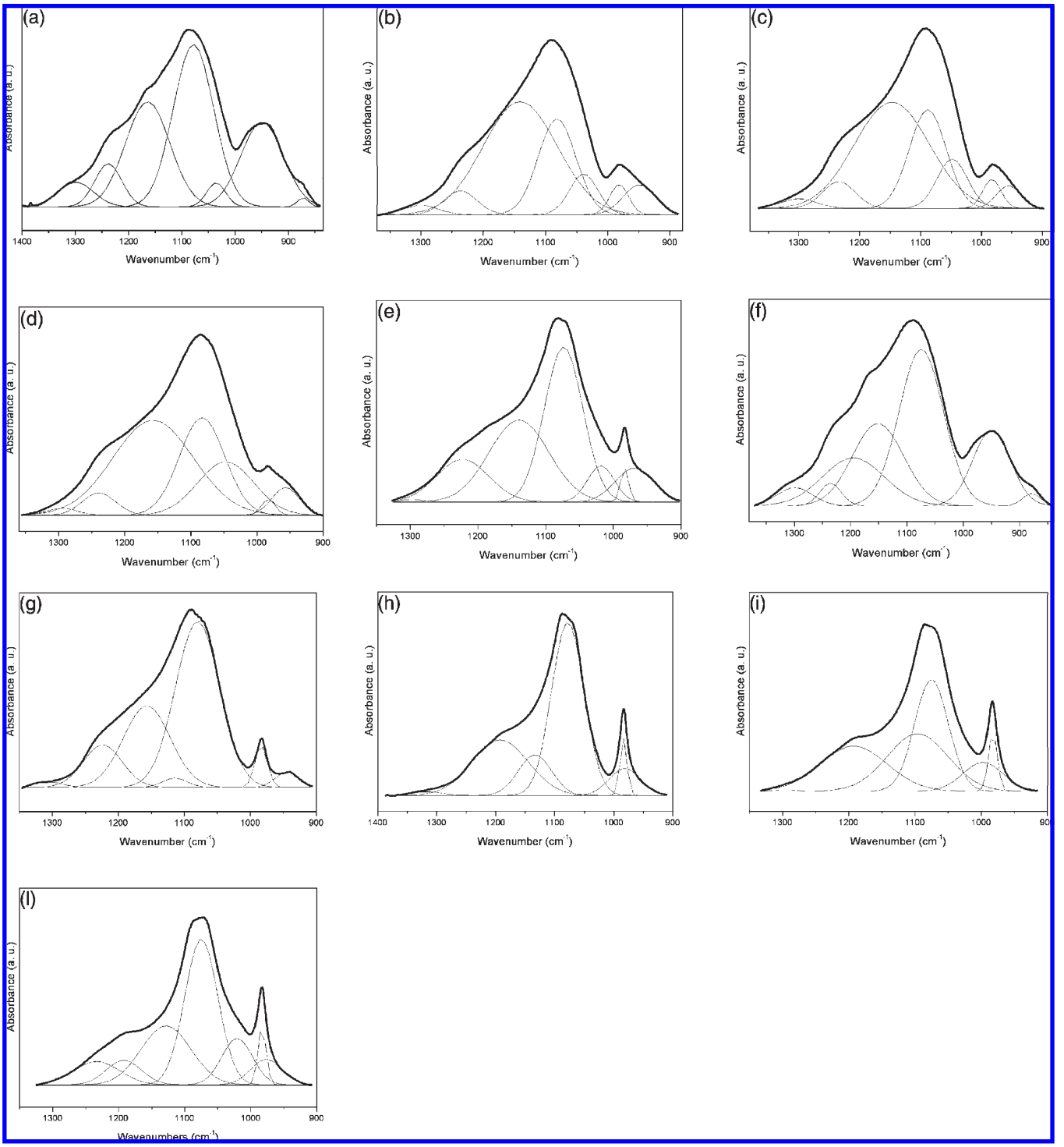

Figure 5. Deconvolution of the Si−O−Si and Si−OH stretching bands of the dried silica obtained at pH 5.45 (a), 6.83 (b), 7.64 (c), 9.38 (d), 10.38 (e) (density 1.03 g/cm^3) and pH 5.42 (f), 6.90 (g), 7.54 (h), 9.33 (i), 10.30 (l) (density 1.09 g/cm^3).

1080 cm^{-1} and 1055 cm^{-1} increase until pH 7 and decrease at higher pH (Table 3). The shift of both components to lower wavenumbers is usually related to a more porous structure, and larger Si−O−Si angles and Si−O bond lengths.[31] The evolution of the bands dooes not seem to be influenced by the density of the metasilicate solution.

The development of the network can be also monitored by following the progression of the band due to the stretching mode of Si−OH (950−980 cm^{-1}). The bands at around 950 cm^{-1} and 980 cm^{-1} are due to stretching of SiO^- and SiOH, respectively. The deconvoluted spectra clearly show that as the pH is increased, the band at 950 cm^{-1} decreases in intensity and disappears and the band at 980 cm^{-1} appears and its intensity increases. The infrared spectra of the composites in the region between 1400 cm^{-1} and 900 cm^{-1} show the same bands of the pure silica together with the characteristic bands of calcium phosphates detected by X-ray analyses. No shifts have been recorded (data not shown).

Morphological Investigation of Calcium Phosphates-Silica Composites. Scanning electron microscopy (SEM) was used

Table 3. Wavenumbers (cm^{-1}) of the Si−O−Si Stretching Modes

mtasilicate solution density (g/cm^3)	5.45	6.83	7.64	9.38	10.28	5.45	pH
1.03	1078	1082	1088	1083	1074	1078	$\upsilon_{Si-O-Si}$ (LO)
	1151	1157	1164	1156	1145	1151	$\upsilon_{Si-O-Si}$ (TO)
mtasilicate solution density (g/cm^3)	5.42	6.90	7.54	9.33	10.30	5.42	pH
1.09	1075	1080	1078	1075	1075	1075	$\upsilon_{Si-O-Si}$ (LO)
	1151	1157	1154	1152	1151	1151	$\upsilon_{Si-O-Si}$ TO)

to study texture and morphology of silica/calcium phosphate composite material. Comparing the two densities, at the same pH values, no difference in the morphology was observed. However, samples texture and morphology appeared very different as a function of pH. Here we report only a few representative examples.

In Figure 6a, a brushite single crystal obtained at pH 5.42 is shown using a metasilicate solution at 1.09 g/cm^3 density. The crystal is about 20 μm long and 10 μm wide. The elongation of the crystal along the *b* axis is in agreement with its preferential orientation observed by the X-ray diffraction analyses. The surface of the crystal appears strongly etched and characterized by the presence of channels and pores. The orientation of the surface channels reflects the growth direction of the crystal (Figure 6b). We suppose that they hosted amorphous porous silica that is still partially present within the crystal, although brushite diffracted as a single crystal (data not reported). Figure 6c shows a single crystal of DCPD precipitated at pH 9.33 using a metasilicate solution at 1.09 g/cm^3 density. The crystal is 100 μm long and 60 μm wide. In Figure 6d, the surface texture of the same sample is reported, showing a plate-like OCP crystals and silica aggregates that cover and/or are embedded in the DCPD crystal.

It is worth noting that both FT-IR and SEM analysis indicate that brushite is coated by amorphous silica layers. Also, some silica is embedded within the crystals. To reveal the surface texture of brushite and confirm the presence of silica coated and/or embedded within the crystals, we selected big brushite crystals from an experiment carried out at gel density 1.03 g/cm^3 and pH 9.38. Then, we submitted them to alkaline dissolution using 5 M NaOH and after to a FESEM investigation.

Figure 7a shows a FESEM micrograph of the surface texture of brushite after alkaline dissolution of the silica. We observe that dissolution of silica at the crystal surface reveals large channels and pores in which remains of silica are still embedded. After this treatment, brushite appears as a big aggregate composed of nanocrystals of 20−40 nm size arranged in layers. The whole ensemble displays edges and angles as a single crystal (Figure 7b).

The above findings are important since they demonstrate that brushite incorporates some silica gel during growth giving rise to a "true composite". This fact is very common during crystallization of macromolecules in silica gel, and for inorganic compounds has been previously described only for calcite.[36]

The transmission electron microscopy (TEM) observations were performed on samples obtained at the two highest pH values at each density. Figure 8a,b shows crystals of HA and a crystal of OCP formed in a gel with 1.03 density and at pH of 9.38 and 10.28, respectively. HA appears as needle-like 100 nm long and 10 nm wide crystals that have the tendency to aggregate along the long axis. The OCP crystal shows that its

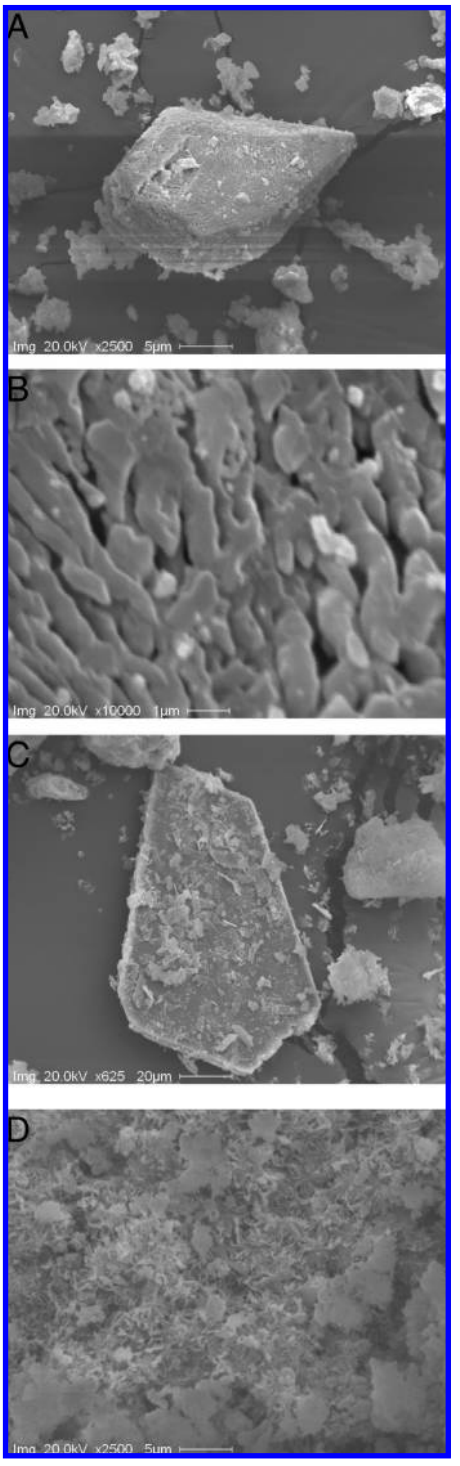

Figure 6. Scanning electron microscope (SEM) pictures of single crystal of brushite (pH 5.42 density 1.09 g/cm^3) (scale bar is 5 μm) (A); texture of the brushite crystal (pH 5.42 density 1.09 g/cm^3) (scale bar is 1 μm) (B); single crystal of brushite (pH 9.33 density 1.09 g/cm^3) (scale bar is 20 μm) (C); surface of the brushite crystal (pH 9.33 density 1.09 g/cm^3) (scale bar is 5 μm) (D).

almost perfectly aligned crystalline domains among which silica is intercalated. The silica appears as sponge-like material.

Figure 8c,d shows the calcium phosphate crystals obtained at the two highest pH values using a metasilicate solution of density 1.09 g/cm^3. At pH 9.33 the HA nanocrystals appear completely coated with unstructured silica and are almost not visible. The same image appears for the OCP crystal

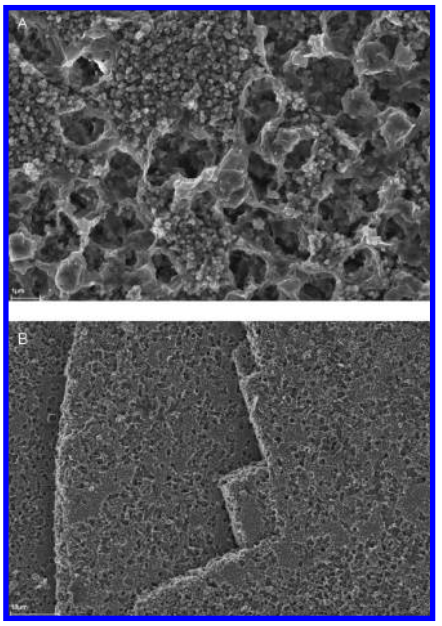

Figure 7. Field emission scanning electron microscope (FESEM) pictures of brushite crystal (pH 9.38 density 1.03 g/cm^3) after alkaline dissolution (scale bars are 1 μm for A and 10 μm for B).

grown at pH 10.30. By comparing the figures, it is possible to see that using the lower density metasilicate solution the resulting calcium phosphates crystals are only partially coated. However, using the higher density metasilicate solution the crystals are completely coated by the silica.

Conclusions

A detailed structural and morphological characterization of different calcium phosphate phases crystallized in silica gel has been performed. Controlled calcium phosphates precipitation has been obtained by a calcium chloride diffusion through metasilicate solutions polymerized at different densities and pHs with phosphoric acid.

The variation of silica gel structure as a function of metasilicate density and pH has been determined basically in terms of silica pores volume and entrapped structural water. According to the literature, at fixed density, the silica structural organization in terms of linear or randomly branched chains formation presents a maximum at around pH 7.0 and two minima at extreme pH values. Subsequently, silica has larger pores at extreme pH, while it is microporous at around pH 7.0. Increasing the experimental densities, an enhancement of the entrapped structural water has been observed. These findings, obtained for dried silica gels, have been correlated to the different calcium phosphates phases obtained as a function of gel pH and density. We have pointed out the possibility at fixed pH value to use the different density of the metasilicate solution in order to obtain HA and DCP instead of OCP and DCPD, respectively. In fact, HA and DCP are dehydrated phases and preferentially grow in silica gels with a low entrapped water content and thus in a more dried environment. The crystallization of HA and DCPD is closely controlled by the pH value. These results appear unexpected if we consider that OCP and DCPD crystallization is favored at about pH 6.0, but we have to consider that the reported pH values are consistent with the starting metasilicate solutions and the local pH inside the gel can be modified by the gel polymerization process and the calcium ions diffusion.

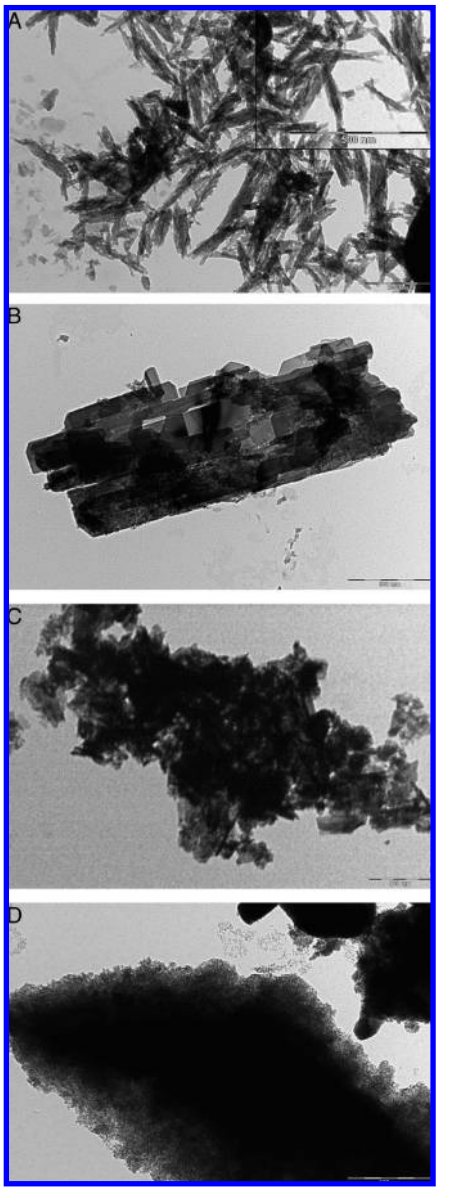

Figure 8. Transmission electron microscopy (TEM) images of calcium phosphates obtained at pH 9.38 (scale bar 200 nm), (inset, scale bar 500 nm) (A), 10.28 (scale bar 500 nm) (B) (density = 1.03 g/cm^3); and pH 9.33 (scale bar 500 nm) (C), 10.30 (scale bar 500 nm) (D) (density = 1.09 g/cm^3).

Brushite has been obtained as a "true composite". Silica layers coat large brushite crystals and at the same time silica is embedded within the crystals during its growth.

Simply by combining the two parameters such as pH and density of the metasilicate solution, it is possible to tailor silica structure, control the growth of calcium phosphate phases, and modulate the amount of silica covering the crystals.

This method represents a straightforward, economic, and controllable system for obtaining functional composite biomaterials. Moreover, this material could lead to significant improvements of the performances of implants in terms of osteointegration, in possible association with the ability to deliver biologically active substances to the target tissues.

Acknowledgment. We thank the Universities of Bologna and Piemonte Orientale (funds for selected research topics), the Italian Ministero dell'Istruzione, Università e Ricerca

(MIUR) and C.I.R.C.M.S.B. (Inter University Consortium for Research on Metal Chemistry in Biological Systems). This work has been supported by bilateral CSIC-CNR project 2007/2008 number 0013890. M.I. is a recipient of a fellowship from Regione Piemonte.

References

(1) Hench, L. L.; Polak, J. M. *Science* **2002**, *295*, 1014.
(2) Lowestan, H. A.; Weiner, S. *On Biomineralization*; Oxford University Press: New York 1989.
(3) López-Macipe, A.; Gómez-Morales, J.; Rodríguez-Clemente, R. *Adv. Mater.* **1998**, *10*, 49.
(4) LeGeros, R. Z. *Calcium Phosphates in Oral Biology and Medicine*; Karger: Basel, Switzerland, 1991.
(5) Ning, C. Q.; Mehta, J.; El-Ghannam, A. *J. Mater. Sci. - Mater. Med.* **2005**, *16*, 355.
(6) Vallet-Regí, M.; Ruiz-González, L.; Izquierdo-Barba, I.; González-Calbet, J. M. *J. Mater. Chem.* **2006**, *16*, 26.
(7) Canullo, L.; Dellavia, C. *Clin. Implant. Dent. Relat. Res.* **2009**, Epub ahead of print.
(8) Villacampa, A. I.; Garcia Ruiz, J. M. *J. Cryst. Growth* **2000**, *211*, 111.
(9) Sousa, A.; Sousa, K. C.; Sousa, E. M. B. *Acta Biomater.* **2008**, *4*, 671.
(10) Roveri, N.; Palazzo, B.; Iafisco, M. *Exp. Opin. Drug Deliv.* **2008**, *5*, 861.
(11) Altomare, A.; Burla, M. C.; Giacovazzo, C.; Guagliardi, A.; Moliterni, A. G. G.; Polidori, G.; Rizzi, R. *J. Appl. Crystallogr.* **2001**, *34*, 392.
(12) Hill, R. J.; Howard, C. J. *J. Appl. Crystallogr.* **1987**, *20*, 467.
(13) McCusker, L. B.; Von Dreele, R. B.; Cox, D. E.; Louer, D.; Scardi, P. *J. Appl. Crystallogr.* **1999**, *32*, 36.
(14) Liesegang, R. E. *Naturwiss. Wochenschr.* **1896**, *11*, 353.
(15) Johnsson, M. S. A.; Nancollas, G. H. *Crit. Rev. Oral Biol. M.* **1992**, *3*, 61.
(16) Miyake, M.; Ishigaki, K.; Suzuki, T. *J. Solid State Chem.* **1986**, *61*, 230.
(17) Curry, N. A.; Jones, D. W. *J. Chem. Soc. A* **1971**, *1971*, 3725.
(18) Jones, D. W.; Cruickshank, D. W. J. *Z. Kristallogr., Kristallgeom., Kristallphys., Kristallchem.* **1961**, *116*, 101.
(19) Beevers, C. A. *Acta Crystallogr.* **1958**, *11*, 273.
(20) Koutsopoulos, S. *J. Biomed. Mater. Res.* **2002**, *62*, 600.
(21) Wang, L.; Nancollas, G. H. *Chem. Rev.* **2008**, *108*, 4628.
(22) Zhan, J.; Tseng, Y.-H.; Chan, J. C. C.; Mou, C.-Y. *Adv. Funct. Mater.* **2005**, *15*, 2005.
(23) Prieto, M.; Fernàndez-Diaz, L.; Lopez-Andrès, S. *J. Cryst. Growth* **1989**, *98*, 447.
(24) Barta, C.; Zemlicka, J. *J. Cryst. Growth* **1971**, *10*, 158.
(25) Roop Kumar, R.; Wang, M. *Mater. Lett.* **2001**, *49*, 15.
(26) Parekh, B.; Joshi, M.; Vaidya, A. *J. Cryst. Growth* **2008**, *310*, 1749.
(27) (a) Brinker, C. J.; Scherer, G. W. *The Physics and Chemistry of Sol-Gel Processing*; Academic Press Inc.: San Diego, CA, USA, 1990. (b) Iler, R. K. *The Chemistry of Silica*; John Wiley & Sons: New York, 1979.
(28) Iler, R. K. *The Chemistry of Silica*; John Wiley & Sons: New York, 1979.
(29) Meixner, D. L.; Dyer, P. N. *J. Sol-Gel Sci. Technol.* **1999**, *14*, 223.
(30) Curran, M. D.; Stiegman, A. E. *J. Non-Cryst. Solids* **1999**, *249*, 62.
(31) Sun, L. N.; Zhang, H. J.; Fu, L. S.; Meng, Q. G.; Peng, C. Y.; Yu, J. B. *Adv. Funct. Mater.* **2005**, *15*, 1041.
(32) Almeida, R.; Pantano, C. *J. Appl. Phys.* **1990**, *68*, 4225.
(33) Fidalgo, A.; Ilharco, L. M. *J. Non-Cryst. Solids* **2001**, *283*, 144.
(34) Lenza, R. F. S.; Vasconcelos, W. L. *Mater. Res.* **2001**, *4*, 175.
(35) Hench, L. L.; West, J. K. *Chem. Rev.* **1990**, *90*, 33.
(36) Prieto, M.; García-Ruiz, J. M.; Amorós, J. L. *J. Cryst. Growth* **1981**, *52*, 864.